Pis'ma v ZhETF, vol. 102, iss. 2, pp. 89 – 93

Strength of solid and molten aluminum under dynamic tension

A. E. Mayer[1)], *P. N. Mayer*

Chelyabinsk State University, 454001 Chelyabinsk, Russia

Submitted 16 March 2015
Resubmitted 17 April 2015

Under dynamic loading, an aluminum melt has a comparable or even higher strength than solid aluminum at room temperature. This phenomenon is possible due to the uniformity of the melt and the homogeneous nucleation of voids within it, whereas the fracture mechanics of a solid are controlled by pre-existing defects. High-current electron irradiation of an initially solid metal plate can be used to observe this effect.

DOI: 10.7868/S0370274X15140039

In everyday life, solids are more capable of withstanding tension than liquids. Intuitively, this is also expected for dynamic loading of a metallic melt. Similar to the case of solid, a tensile strength of melt can be introduced as the maximal absolute value of negative pressure realized in melt under dynamic expansion before its fracture due to cavitation. It seems natural that the melt should always have less tensile strength than the corresponding solid metal. In this paper, we analyze a possible situation for aluminum in which the melt has a comparable or even higher dynamic tensile strength than the solid metal. Our analyses are based on data from experiments [1–4] and molecular-dynamics (MD) simulations [5, 6], as well as the results of our modeling. In addition, we propose a schematic for an experiment, which can be used to make measurements of the dynamic tensile strength of the molten aluminum and to observe the reported effect. This topic is not only of interest to academics, but is also of practical importance due to developing high energy density technologies.

To determine the dynamic strength of solid aluminum, we used data from high-speed impact experiments [1–3], intensive ultra-short laser irradiation [4], MD simulations [5, 6], and results of our MD simulations using LAMMPS [7] package and the potential of interatomic interactions from [8]. In our MD simulations, the uniform uniaxial tension was modeled by the scaling of coordinates of atoms, which simulates the inertial expansion of melt typical for experimental situations (in experiments, previously compressed or heated layer firstly expands due to the pressure gradients, and then due to inertia). The system was deformed in a Nose–Hoover thermostat at the constant temperature and with the relaxation time of 0.1 ps (time step is 0.001 ps). Additional calculations in adiabatic conditions showed that the tensile strength depends only on temperature at the moment of fracture. On the other hand, current temperature depends on prehistory of deformation (e.g., previous compression). Therefore, in order to have reference points, we considered the constant temperature. Periodic boundary conditions were set for all boundaries. The system was chosen large enough to ensure independence of calculated strength on the system size: the number of atoms varied from about 100 000 to 4 millions depending on the strain rate. Relaxation at zero pressure during 5 ps occurred prior to tension. Temporal dependences of average longitudinal stresses in the MD system were analyzed. All data for strength of solid aluminum are collected in Fig. 1. One can see a correspondence between our MD simulations and the existing experimental [4] and calculated [5, 6] data for solid aluminum.

According to [4, 9], the tensile strength is a power function of the tension rate. According to [10, 11], there are two modes of fracture for solid metals: i) a heterogeneous mode, in which the damage develops from existing defects within the material (pores, microcracks), and ii) a homogeneous mode, which is realized if the concentration of the pre-existing defects is insufficient to cause failure, so that all the volume of the material takes a part in the generation of new voids from stochastic fluctuations. The transition from mode i to mode ii occurs at strain rates higher than 10^8–$10^9\,\mathrm{s}^{-1}$. This transition is characterized by a substantial drop in the strain rate sensitivity of the tensile strength. The homogeneous nucleation mode with a low strain rate sensitivity of strength corresponds to the usual behavior observed in MD simulations (see Fig. 1). In any case, the dynamic strength of solid aluminum increases from a value of approximately 2 to 6–8 GPa as the strain rate increases from $\sim 10^6$ to $\sim 10^9 - 10^{10}\,\mathrm{s}^{-1}$, as previous experiments have shown.

[1)]e-mail: mayer@csu.ru

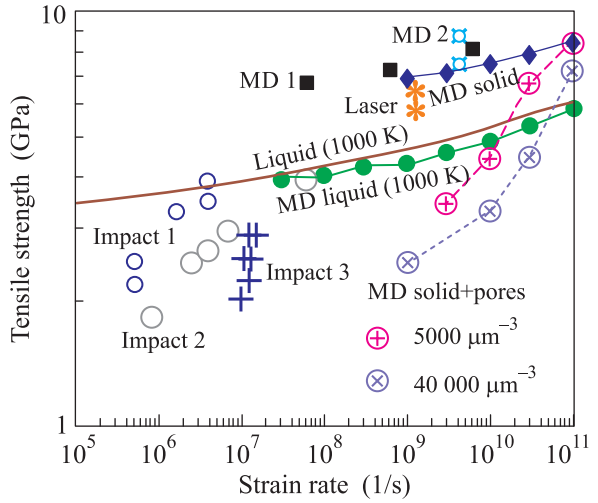

Fig. 1. Strain rate dependencies of the tensile strength of solid and molten aluminum: monocrystalline aluminum (small rings "impact 1" – impact experiments [3]; filled squares "MD 1" and figured rings "MD 2" – MD simulations of [6] and [5], respectively; rhombs with line "MD solid" – our MD simulations at 300 K), polycrystalline aluminum (large rings "impact 2" and daggers "impact 3" – impact experiments [1] and [2], respectively; asterisks "laser" – laser experiments [4]), solid aluminum at 300 K with pores (markers with line "MD solid + pores" present our MD simulations, diameter of pores is 5 nm, concentrations are 5 000 and 40 000 per cubic micrometer; porosities are 0.09 and 0.7 %, respectively) and homogeneous molten aluminum at 1000 K (solid line "liquid (1000 K)" – our calculations using the model [12], filled circles with line "MD liquid (1000 K)" – our MD simulations). Our MD simulations for solid and liquid aluminum are made with use of LAMMPS [7] and the interatomic potential [8]

For super-high strain rates ($\geq 10^8\,\mathrm{s}^{-1}$), the tensile strength of the melt at 1000 K is determined from the results of our MD simulations (see Fig. 1). The LAMMPS [7] package is also used with the potential of interatomic interactions from [8]. To analyze the tensile strength of the aluminum melt in a wider range of strain rates, we used a model [12] based on the classical theory of a metastable liquid [13]. The homogeneous nucleation and growth of spherical voids in the melt at negative pressures are considered in this model. The growth of the voids is described by the Rayleigh–Plesset equation [14] and the thermal fluctuations [15] provide the nucleation for super-critical voids, which are able to grow at a given negative pressure. The maximum absolute value of the negative pressure is when the growth rate of the volume of the voids is equal to the growth rate of the volume of the melt. This maximum value is the tensile strength of the melt at the given strain rate and temperature. The calculated strain rate dependence of the tensile strength of the aluminum melt at 1000 K is shown in Fig. 1. In these calculations, we take into account the size distribution of the voids (all voids are divided into generations according to the time of nucleation). We used data [16] for surface tension, data [17] on viscosity of the melt, and the wide-range equation of state [18] to determine the thermodynamic parameters of the melt. One can see a close fit between the model [12] and MD in the range of strain rates $\geq 10^8\,\mathrm{s}^{-1}$, where MD simulation makes sense.

Fig. 1 demonstrates our main idea. At super-high strain rates, the strength of the solid metal is higher than the strength of the melt, which is confirmed from MD simulations result and laser experiments. At strain rates less than $\sim 5 \cdot 10^7\,\mathrm{s}^{-1}$, the tensile strength of the melt becomes higher than the strength of the polycrystals. When the strain rate decreases to less than $\sim 5 \cdot 10^6\,\mathrm{s}^{-1}$, the melt becomes more durable than the monocrystalline aluminum. This phenomenon is due to a weak rate sensitivity of the strength of the melt in the homogeneous nucleation mode, whereas the solid metal transitions to the heterogeneous fracture mode and its rate sensitivity sharply increases. Therefore, a higher melt strength may be achieved if the homogeneous nucleation mode occurs in the melt over the strain rate range from 10^6 to $10^8\,\mathrm{s}^{-1}$.

In order to argue our idea, Fig. 1 also presents MD simulation results of uniaxial tension with the constant strain rate of aluminum with high concentration (5 000 and 40 000 per cubic micrometer) of small pores (with diameter of 5 nm). Simulation conditions were similar to the cases of solid aluminum without defects and aluminum melt considered before. Initial pore and the void formed in the course of deformation are imaged in Fig. 2 (the program Ovito [19] was used for visualization). One can see a sharp drop of the tensile strength with the strain rate decrease in the case of solid metal with pores in Fig. 1. Difference in strength of perfect monocrystal and porous solid aluminum grows up with the strain rate decrease. The strength of our models of porous material becomes less than the melt strength at the strain rates $< 5 \cdot 10^{10}$ and $< 1 \cdot 10^{10}\,\mathrm{s}^{-1}$ depending on concentration of pores. It means that softening due to the presence of defects (pores) is more substantial than the thermal softening. On the other hand, one can see in Fig. 1 the transition to homogeneous mode of fracture for porous aluminum with concentration of pores of 5 000 per cubic micrometer at the strain rate of $10^{11}\,\mathrm{s}^{-1}$ – the tensile strengths of porous and perfect aluminum coincide at such strain rate. Calculations show that a decrease

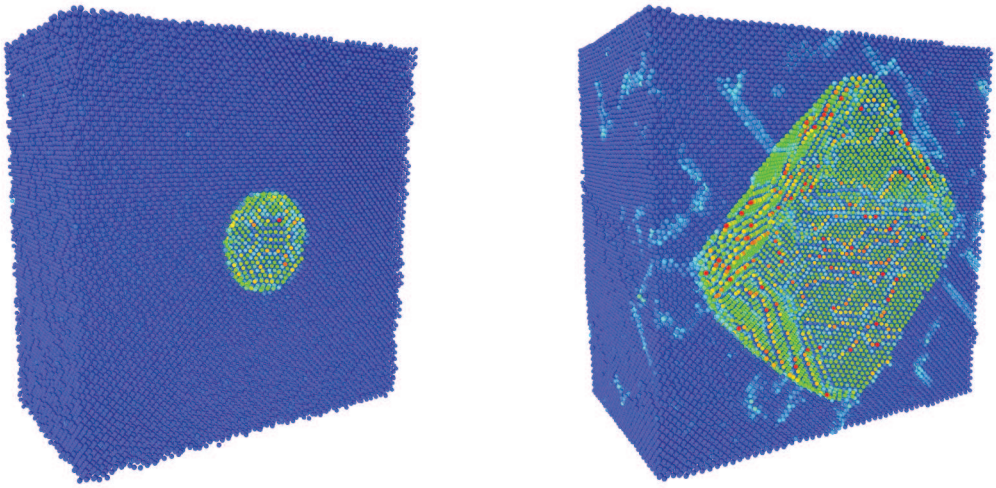

Fig. 2. (Color online) Initial pore and void formed at late stage of deformation; aluminum, temperature is 300 K, strain rate is $10^9\,\mathrm{s}^{-1}$. Color corresponds to the value of centro-symmetry parameter; visualization with use of Ovito [19]

of the pore concentration leads to a shift of the considered strength drop in the direction of smaller strain rates. Therefore, the transition between homogeneous and heterogeneous modes of fracture accompanied by the strength drop substantially depends on the concentration of initial defects. The samples examined in experiments [1–3] (the strength drop in the range from 10^5 to $10^8\,\mathrm{s}^{-1}$) should have concentrations of pores (or other similar defects) on the orders of magnitude smaller than in our MD models of porous aluminum. Pores in solid metal are stable (at least, on the considered time scale), while MD simulations with melt show that the pores of 5 nm in diameter are healed during 5 ps at zero pressure in the system. Therefore, artificial introduction of the same pores do not alter the tensile strength of the melt, if only the melt has 5 ps to relax before tension.

The homogeneous fracture mode occurs if the concentration of pre-existing cavities (bubbles) in the melt is small. This amount should be much smaller than the concentrations of voids, which are generated in a uniform melt due to the homogeneous nucleation at a given strain rate. Fig. 3a shows the strain rate dependencies on the concentration of voids and the minimum critical void diameters for the homogeneous nucleation mode calculated using the model [12]. The critical diameter varies slowly as the strain rate increases and is of the order of a nanometer. The formation of cavities of this size may occur as a result of thermal fluctuations. This means that even small pre-existing cavities can influence the strength if the concentration is comparable with the concentration shown in Fig. 3a. At super-high strain rates ($> 10^8\,\mathrm{s}^{-1}$) the concentration of pre-existing cavities should be high (> 10 per cubic micrometer). Therefore, homogeneous nucleation is predominant for these conditions, and the melt can be treated as uniform. Vice versa, at low and moderate strain rates ($< 10^5\,\mathrm{s}^{-1}$), even a small number of pre-existing bubbles (< 10 per cubic millimeter) will substantially influence the strength. Therefore, it is very hard to have the homogeneous nucleation mode at such strain rates.

From the data presented in Fig. 3a, the possibility to observe a high tensile strength of melt depends substantially on the initial state of the melt prior to the application of tension. Surface tension and fluidity of the melt positively influence its homogeneity. The surface tension leads to the collapse of bubbles and positive pressure reduces the time required for collapse (see Fig. 3b). According to the data presented in Fig. 3b, maintaining the melt at a pressure of about several GPa over a period of 10–100 ns can lead to the collapse of even those bubbles with an initial diameter of ~ 0.1 mm. If the negative pressure is applied after this period, the homogeneous nucleation mode can be observed, and the strength of the melt can exceed the strength of the solid metal. In solid metal, the healing of pores and other defects is suppressed by the elastic stresses (the tendency of solids to hold their original shape). According to some experimental data [20, 21], the preliminary action of the increased pressure leads to the strengthening of the solid metal as well. If this is the case, it may be interpreted as a gradual transition from the heterogeneous to the homogeneous fracture mode at the expense of the collapse of pre-existing defects as a result of the applied pressure, which is similar to the case observed for the melt.

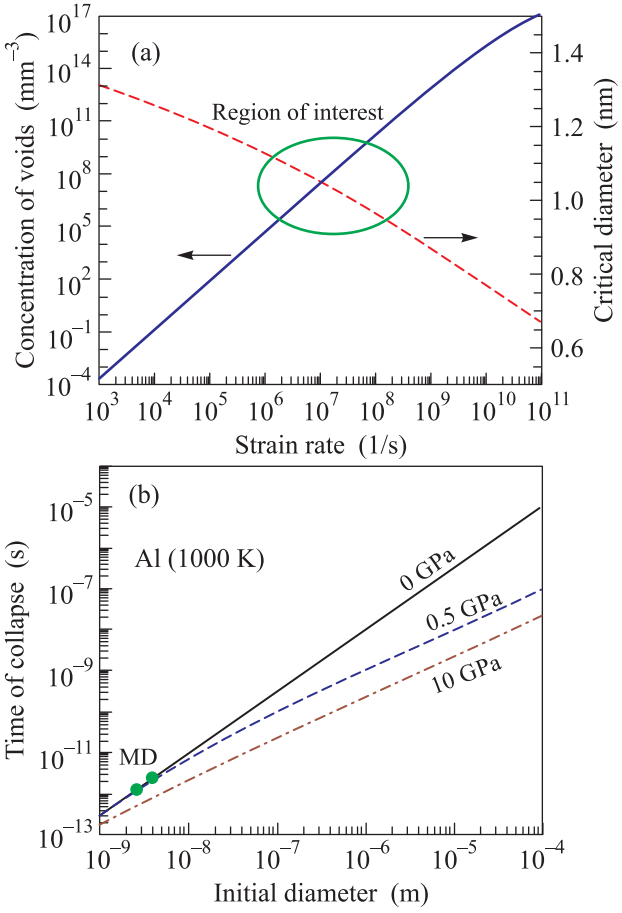

Fig. 3. (a) – Strain rate dependencies of the total concentration of voids (solid line, left scale) and the minimum diameter of the critical voids (dashed line, right scale); (b) – Dependencies of time of collapse of the pre-existing bubbles on the initial radius at zero pressure in the melt (solid line) and at positive pressures (dashed lines). Solid circles "MD" are estimations from MD simulations at zero pressure. Other calculations were performed with use of the model [12]

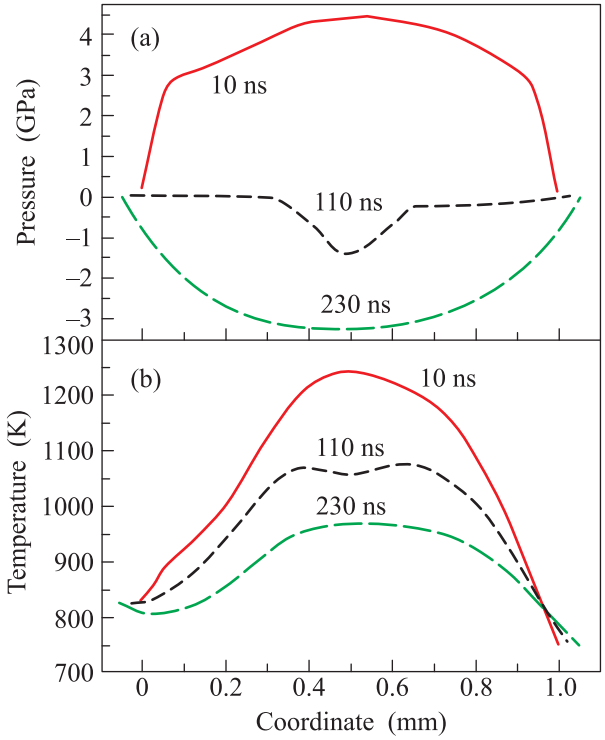

Fig. 4. Spatial distributions of the pressure (a) and the temperature (b) in the aluminum target (initial thickness of 1 mm) after irradiation using a high-current electron beam with a pulse duration of 10 ns, a current density of 25 kA/cm^2, and an electron energy of 1 MeV (calculations were performed using the CRS [27] code)

As a thought exercise, let us discuss the possibility of performing an experimental measurement of the tensile strength of the melt and observing the discussed effect. The action of ultra-short pulses of powerful laser irradiation [22–25] can cause heating, melting, and subsequent expansion of the heated layer. From this, the spall fracture of the melt can be observed and its tensile strength can be determined [23]. The values of the melt strength determined in [23] correspond to the results from calculations regarding the use of the homogeneous nucleation model [12]. For ultra-short laser irradiation, the strain rates ($\geq 10^9\,\mathrm{s}^{-1}$) transcend the upper limit of our region of interest (10^6–$10^8\,\mathrm{s}^{-1}$). Using high-current electron irradiation with nanosecond durations [26] seems to be more promising. Fig. 4 shows results of our calculations using the CRS [27] computer code and include: the spatial distributions of the pressure (Fig. 4a) and the temperature (Fig. 4b) in the aluminum target with a thickness of 1 mm after an electron beam irradiation with an electron energy of 1 MeV, a current density of 25 kA/cm^2, and a duration of 10 ns. In this case, the range of fast electrons exceeds the target thickness, meaning that the entire target volume is heated. The target material does not have enough time for expansion during the irradiation pulse, meaning that the heating takes place at an almost constant volume. The main thermal expansion takes place after the irradiation, and the following expansion due to inertial effects leads to the formation of a melt state with the negative pressure. In the considered example, the molten aluminum is kept at a positive pressure (up to 4 GPa) over a period of ~ 80 ns, which serves to heal any pre-existing pores (see Fig. 3b). Afterwards, the molten aluminum at the center of the target is subjected to a tensile stress (up to 3.2 GPa) at a strain rate of $\sim 10^6\,\mathrm{s}^{-1}$, which corresponds to the tensile strength for the homogeneous nucleation mode (see Fig. 1). In these experiments, var-

ious tensile stress levels and melt temperatures can be obtained by the preliminary heating of target and by varying the current density. Using laser registration of the free surface velocity [9] is appropriate for detecting if the melt experiences fracture.

In this work, our analysis reveals that over the range of strain rates of 1–100 per microsecond, it is possible to achieve a homogeneous cavitation mode in an aluminum melt under tension, at which the tensile strength of the melt is comparable or even higher than the strength of the solid aluminum at room temperature. The required loading conditions can be obtained by irradiating a solid target by a high-current electron beam with an electron energy of ~ 1 MeV and a pulse duration of tens of nanoseconds. Such setup can be used for experimental measurements of the tensile strength of the aluminum melt and for observations of the discussed effect. Our MD calculation of the tensile strength of porous aluminum shows that softening due to presence of defects (pores) can be more substantial than thermal softening. In addition to the theoretical interest of this topic, our results may have a significant influence on the development of the high-energy density devices, in which a liquid shell may prove to be stronger than a solid one.

The work is supported by a grant from the Russian Science Foundation (Project # 14-11-00538).

1. G. I. Kanel, S. V. Razorenov, A. V. Utkin, K. Baumung, H. U. Karov, and V. Licht, AIP Conf. Proc. **309**, 1043 (1994).
2. E. Moshe, S. Eliezer, E. Dekel, A. Ludmirsky, Z. Henis, M. Werdiger, I. B. Goldberg, N. Eliaz, and D. Eliezer, J. Appl. Phys. **83**, 4004 (1998).
3. G. I. Kanel, S. V. Razorenov, K. Baumung, and J. Singer, J. Appl. Phys. **90**, 136 (2001).
4. S. I. Ashitkov, M. B. Agranat, G. I. Kanel, P. S. Komarov, and V. E. Fortov, JETP Lett. **92**, 516 (2010).
5. V. V. Zhakhovskii, N. A. Inogamov, Yu. V. Petrov, S. I. Ashitkov, and K. Nishihara, Appl. Surf. Sci. **255**, 9592 (2009).
6. P. A. Zhilyaev, A. Yu. Kuksin, V. V. Stegailov, and A. V. Yanilkin, Phys. Sol. State **52**, 1619 (2010).
7. S. Plimpton, J. Comput. Phys. **117**, 1 (1995).
8. X. W. Zhou, H. N. G. Wadley, R. A. Johnson, D. J. Larson, N. Tabat, A. Cerezo, A. K. Petford-Long, G. D. W. Smith, P. H. Clifton, R. L. Martens, and T. F. Kelly, Acta Mater. **49**, 4005 (2001).
9. G. I. Kanel', V. E. Fortov, and S. V. Razorenov, Phys.–Usp. **50**, 771 (2007).
10. A. E. Mayer, in *Proc. 13th Int. Conf. on Fracture*, paper # S12-012, Beijing (2013).
11. A. E. Mayer, K. V. Khishchenko, P. R. Levashov, and P. N. Mayer, J. Appl. Phys. **113**, 193508 (2013).
12. P. N. Mayer and A. E. Mayer, ZhETF **148**(1), 42 (2015).
13. V. P. Skripov, *Metastable Liquids*, Wiley, N.Y. (1974).
14. A. Yu. Kuksin, G. E. Norman, V. V. Pisarev, V. V. Stegailov, and A. V. Yanilkin, Phys. Rev. B **82**, 174101 (2010).
15. L. D. Landau and E. M. Lifshitz, *Course of Theoretical Physics, Vol. 5. Statistical Physics. Part 1*, Butterworth-Heinemann, Oxford (1980).
16. H. M. Lu and Q. Jiang, J. Phys. Chem. B **109**, 15463 (2005).
17. J. H. Hildebrand and R. H. Lamoreaux, Proc. Natl. Acad. Sci. U. S. A. Chemistry **73**, 98 (1976).
18. S. N. Kolgatin and A. V. Khachatur'yants, Teplofiz. Vys. Temp. **20**, 90 (1982).
19. A. Stukowski, Modell. Simul. Mater. Sci. Eng. **18** 015012 (2010).
20. S. A. Abrosimov, A. P. Bazhulin, V. V. Voronov, I. K. Krasyuk, P. P. Pashinin, A. Yu. Semenov, I. A. Stuchebryukhov, and K. V. Khishchenko, Dokl. Phys. **57**, 64 (2012).
21. S. A. Abrosimov, A. P. Bazhulin, V. V. Voronov, A. A. Geras'kin, I. K. Krasyuk, P. P. Pashinin, A. Yu. Semenov, I. A. Stuchebryukhov, K. V. Khishchenko, and V. E. Fortov, Quantum Electron. **43**, 246 (2013).
22. M. E. Povarnitsyn, T. E. Itina, M. Sentis, K. V. Khishchenko, and P. R. Levashov, Phys. Rev. B **75**, 235414 (2007).
23. M. B. Agranat, S. I. Anisimov, S. I. Ashitkov, V. V. Zhakhovskii, N. A. Inogamov, P. S. Komarov, A. V. Ovchinnikov, V. E. Fortov, V. A. Khokhlov, and V. V. Shepelev, JETP Lett. **91**, 471 (2010).
24. B. J. Demaske, V. V. Zhakhovsky, N. A. Inogamov, and I. I. Oleynik, Phys. Rev. B **82**, 064113 (2010).
25. M. Gill-Comeau and L. J. Lewis, Phys. Rev. B **84**, 224110 (2011).
26. E. F. Dudarev, A. B. Markov, A. E. Mayer, G. P. Bakach, A. N. Tabachenko, O. A. Kashin, G. P. Pochivalova, A. B. Skosyrskii, S. A. Kitsanov, M. F. Zhorovkov, and E. V. Yakovlev, Russ. Phys. J. **55**, 1451 (2013).
27. A. E. Mayer, E. N. Borodin, V. S. Krasnikov, and P. N. Mayer, J. Phys.: Conf. Ser. **552**, 012002 (2014).